INFECTION AND IMMUNITY, July 2002, p. 3824–3832 Vol. 70, No. 7
0019-9567/02/$04.00+0 DOI: 10.1128/IAI.70.7.3824–3832.2002

Fluorescence Resonance Energy Transfer Microscopy of the *Helicobacter pylori* Vacuolating Cytotoxin within Mammalian Cells

David C. Willhite, Dan Ye, and Steven R. Blanke*

Department of Biology and Biochemistry, University of Houston, Houston, Texas 77204-5001

Received 29 January 2002/Returned for modification 7 March 2002/Accepted 11 April 2002

The *Helicobacter pylori* vacuolating cytotoxin (VacA) binds and enters mammalian cells to induce cellular vacuolation. To investigate the quaternary structure of VacA within the intracellular environment where toxin cytotoxicity is elaborated, we employed fluorescence resonance energy transfer (FRET) microscopy. HeLa cells coexpressing full-length and truncated forms of VacA fused to cyan fluorescent protein (CFP) or yellow fluorescent protein (YFP) were analyzed for FRET to indicate direct associations. These studies revealed that VacA-CFP and VacA-YFP interact within vacuolated cells, supporting the belief that monomer associations at an intracellular site are important for the toxin's vacuolating activity. In addition, the two fragments of proteolytically nicked VacA, p37 and p58, interact when coexpressed within mammalian cells. Because p37 and p58 function in *trans* when expressed separately within mammalian cells, these data suggest that the mechanism by which these two fragments induce vacuolation requires direct association. FRET microscopy also demonstrated interactions between mutant forms of VacA, as well as wild-type VacA with mutant forms of the toxin within vacuolated cells. Finally, a dominant-negative form of the toxin directly associates with wild-type VacA in cells where vacuolation was not detectable, suggesting that the formation of complexes comprising wild-type and dominant-negative forms of toxin acts to block intracellular toxin function.

Persistent infection of the human gastric mucosa with the gram-negative pathogen *Helicobacter pylori* is responsible for chronic inflammation that can result in peptic ulcer disease or stomach cancer (2, 4, 6, 33, 34, 43, 46, 57). Pathogenic strains of *H. pylori* secrete a vacuolating cytotoxin (VacA) that induces the formation of large intracellular vacuoles within gastric epithelial cells both in vitro and in vivo, presumably by causing a defect in vesicular trafficking (3, 29). Oral administration of purified VacA to mice results in degeneration of the gastric mucosa and inflammatory cell recruitment, characteristic of *H. pylori*-mediated diseases (23, 32). VacA was recently reported to be important for colonization of *H. pylori* within a mouse model (53). While increasing evidence supports the view that VacA is an important virulence factor in *H. pylori*-mediated gastric ulcer disease, the cellular intoxication mechanism of VacA remains poorly understood.

VacA exhibits cellular behavior similar to that of protein toxins that must enter target cells to elaborate cytotoxicity. Mature VacA is organized into an amino-terminal domain (p37; residues 1 to 311) and a carboxyl-terminal domain (p58; residues 312 to 821) that are connected by a protease-sensitive loop (11, 49, 55, 57). The p58 domain contains binding determinants within residues 480 to 700 that facilitate VacA interactions at the plasma membrane of sensitive mammalian cells (1, 44, 60). The toxin binds and enters sensitive mammalian cell lines by a slow, temperature-dependent process (22, 36, 51) and has been reported in the cytosol (22) and in membrane-bound vacuoles formed by the toxin (56), as well as in mitochondria (21, 26). Earlier studies showed that determinants from both p37 and p58 were essential for vacuolating activity when truncated fragments of VacA were introduced directly into mammalian cells and tested for their ability to induce vacuolation of cultured monolayers (15, 65). Yeast two-hybrid analyses revealed that VacA interacts with Rack1 (25), as well as with a novel intracellular factor associated with the intermediate filament protein vimentin (16). While these data strongly suggest that VacA elaborates its cytotoxic effects from within mammalian cells, the toxin's biochemical activity responsible for cellular vacuolation has not been elucidated.

Identification of the active form of VacA within the complex milieu of the cytosol would provide important clues for investigating the toxin's biochemical activity. Purified VacA is a monomer under acidic or alkaline conditions that strongly potentiate the toxin's vacuolating activity (9, 17, 40, 63). Since both bacterium-associated VacA and bacterial culture filtrates containing the toxin do not require activation to vacuolate cells (10, 12, 29, 47, 52), it is possible that toxin monomers may be the active form of VacA that is readily present in vivo at the human gastric epithelium. Alternatively, VacA may assemble into a complex requiring intermolecular associations between two or more VacA monomers. In solution, VacA is purified as large oligomeric structures comprising 6 to 14 monomers (7, 9, 35, 59), but it is not clear whether VacA exists as a higher-order structure within intact cells.

The overall objective of this study was to investigate VacA structure in the environment where the toxin elaborates its cytotoxic effects. Specifically, our goal was to distinguish whether VacA is a monomer or a complex of associating monomers within intact vacuolated cells. Recently, fluorescence resonance energy transfer (FRET) microscopy has been employed to investigate protein-protein interactions between red- and blue-shifted variants of green fluorescent protein (GFP) fused to suspected interacting partners within intact

* Corresponding author. Mailing address: Department of Biology and Biochemistry, University of Houston, 369 Science & Research Building II, Houston, TX 77204-5001. Phone: (713) 743-8392. Fax: (713) 743-8351. E-mail: sblanke@uh.edu.

mammalian cells (13, 18, 28, 31, 62). FRET microscopy is a powerful approach for detection of protein-protein interactions without disruption of the cells or artificial nuclear localization; for a review, see reference 48. FRET occurs when the emission spectrum of one fluor (the donor) overlaps with the excitation spectrum of a second fluor (the acceptor) and when energy from excitation of the donor is transferred to the acceptor through quantum effects. FRET is characterized by an increased emission at the acceptor's optimal emission wavelength when excited at the donor's optimal excitation wavelength. The distance, spectral overlap, and the orientation between the two fluors determine efficiency of energy transfer. We have adapted FRET microscopy to investigate interactions between discrete monomers and fragments of VacA. We genetically fused either yellow fluorescent protein (YFP) or cyan fluorescent protein (CFP) to the VacA carboxyl terminus and introduced both wild-type and mutant forms of these fusion proteins into mammalian cells. Collectively, our data indicate that VacA monomers associate within vacuolated mammalian cells, suggesting that intermolecular interactions between discrete monomers are critical for toxin intracellular activity.

MATERIALS AND METHODS

Materials. Restriction enzymes and T4 DNA ligase were purchased from New England Biolabs (Beverly, Mass.). FailSafe DNA polymerase and buffers for PCR were from Epicentre (Madison, Wis.). Oligonucleotides were synthesized by Operon Technologies (Alameda, Calif.). The big-dye terminator cycle sequencing premix kit from Amersham-Pharmacia Biotech (Piscataway, N.J.) was used for sequencing. The plasmids pET20b+ and pET26b+ were obtained from Novagen (Madison, Wis.). Fluorescent protein encoding vectors pEYFP and pECFP-C1, anti-GFP (which also cross-reacts with CFP or YFP), and the CalPhos DNA transfection kit were purchased from Clontech (Palo Alto, Calif.). Vaccinia virus expressing T7 polymerase (ATCC 2153-VR) and *H. pylori* strain 60190 (ATCC 49503) were purchased from the American Type Culture Collection (Manassas, Va.). Antihemagglutinin (anti-HA) and protein G-agarose beads were from Pierce (Rockford, Ill.). [^{35}S]methionine was purchased from DuPont NEN (Wilmington, Del.). Cell culture medium, fetal calf serum, and neutral red were purchased from Gibco BRL (Rockville, Md.). Cell culture plastic ware was from Corning (Cambridge, Mass.), and the eight-well Lab-Tek chamber slides were purchased from Nalge Nunc International (Naperville, Ill.). The triamide signal amplification kit with Alexa Fluor 568 was purchased from Molecular Probes (Eugene, Oreg.). Fluorescence microscopy filters were obtained from Chroma Technologies (Brattleboro, Vt.). Image Gauge V3.0 software from Fuji (Tokyo, Japan) was used for image analysis.

Preparation of plasmids encoding VacA and VacA fragments. Standard and commercial protocols were used for isolation of plasmid DNA, restriction endonuclease digestions, PCR, and cloning (54). The genes encoding YFP and CFP were amplified using pEYFP and pECFP-C1 as template DNA. The primers used to amplify both CFP and YFP were chemically synthesized DNA oligonucleotides with the following sequences: 5′-CTAAGTAGATCTTGGATCCACC ATGGTGAGCAAGGGC-3′ and 5′-CGATGTGAATTCGACTCGAGCTTGT ACAGCTCGTCCA-3′. The amplified DNA fragments encoding CFP and YFP were digested using *Bgl*II and *Eco*RI, generating restriction sites compatible for ligation into *Bam*HI and *Eco*RI sites, respectively. The restricted fragments encoding CFP or YFP were ligated into pET20b+ or pET26b+, replacing the *Bam*HI-*Eco*RI fragment of each plasmid, resulting in pET20b-CFP and pET26b-YFP, respectively.

The genes encoding VacA and fragments of VacA were excised by treating previously described pET20-based plasmids (65) with *Nde*I and *Nco*I. Fragments encoding residues 1 to 311 (p37), 311 to 741 (p58 with residues 742 to 821 removed), 312 to 821 (p58), 1 to 741 (VacA with residues 742 to 821 removed), or 1 to 821 (mature VacA) were ligated into pET20b-CFP or pET26b-YFP, replacing the *Nde*I-*Nco*I fragment of each of these plasmids and thereby yielding in-frame carboxyl-terminal fusions to either CFP or YFP. Plasmids harboring genes encoding full-length VacA or VacA fragments were sequenced across the entire open reading frame.

In vitro transcription and translation and antibody affinity tag immunoprecipitation. We performed in vitro transcription and translation of the VacA fragments in the presence of [^{35}S]methionine using the Promega TNT reticulocyte lysate kit. Fifty-microliter reaction volumes, including 3 μl of each reaction, were run on sodium dodecyl sulfate–12% polyacrylamide gel electrophoresis (SDS–12% PAGE) and were imaged using a Fuji phosphorimager. Target and bait proteins were added in equal molar ratios as calculated from pixel analysis, and the volume was brought to 400 μl with phosphate-buffered saline (PBS) in an Eppendorf tube and then incubated at room temperature for 30 min on an orbital rotator. In order to induce full-length VacA to assume the monomer state and allow reformation as a hetero-oligomer, 100 μl of 50 mM morpholineethanesulfonic acid-gluconate, pH 5.0, was added to HA-VacA + VacA-GFP and HA-p37 + p37-GFP immunoprecipitations, incubated at 25°C for 30 min, and reneutralized using 20 μl of 1 M Tris, pH 7.2, prior to addition of PBS to a 400-μl final volume. Anti-HA or anti-GFP antibody (5 μl) and 10 μl of protein G or protein A beads were mixed and then incubated on an orbital rotator for 30 min. Samples were centrifuged for 1 min at 10,000 × *g*, and supernatant was removed. The pellets were washed four times with 400 μl of Tris-buffered saline–Tween (20 mM Tris, pH 8.0, 25 mM NaCl, and 0.2% Tween 20). After the last wash, samples were resuspended in Laemmli loading buffer containing 0.5% SDS and 1 mM β-mercaptoethanol, incubated at 90°C for 10 min, fractionated by SDS–12% PAGE, and imaged using a Fuji phosphorimager after overnight exposure to a phosphorimaging plate.

Cell culture. HeLa cells were cultured as monolayers in 25-ml plastic flasks in Dulbecco's minimal essential medium containing 10% fetal calf serum under 5% CO_2 at 37°C. Twenty-four hours prior to transfection, HeLa cells were seeded at 2×10^4 cells/well in eight-well microscopy slides or at 1×10^4 cells/well in 96-well plates.

Mammalian cell transfection. Vaccinia virus bearing the T7 RNA polymerase gene (vT7) (20) was thawed and 0.5 volumes of 1-μg/ml trypsin was added. Tubes were vortexed; their contents were incubated at 37°C for 30 min and then applied to HeLa cells in Dulbecco's minimal essential medium (14). DNA was precipitated by adding 6.2 μl of 2 M $CaCl_2$ to 2 μg of each plasmid and by bringing the mixture to 50 μl with distilled and/or deionized water. The DNA solution was added dropwise to 50 μl of 100 mM HEPES buffer (pH 7.4) while being gently vortexed and was then incubated at room temperature for 20 to 40 min (54). After 30 min of incubation with vT7, HeLa cells were washed twice with PBS, 400 μl of fresh medium was applied, and then 20 μl of the calcium phosphate precipitate was added in a dropwise fashion. The cells with DNA precipitate were incubated under 5% CO_2 at 37°C for 2 h. The monolayers were washed twice with PBS, and then 400 μl of medium was replaced and incubated under 5% CO_2 at 37°C overnight.

Vacuolation assay. We quantified relative vacuolation based on the uptake of the dye neutral red within mammalian cells as described previously (10). The experiments were performed in 96-well plates, and neutral red uptake was determined using a Dynatech MR5000 microtiter plate reader to measure the absorbance at 530 nm (minus the absorbance at 410 nm).

Fluorescence imaging. The samples were protected from light, and images were captured quickly (to avoid photo bleaching) using a 40× objective lens on an Olympus BX-60 microscope, resulting in images collected at ×400 total magnification. Cotransfected species were identified by cellular fluorescence under both the CFP and YFP filter sets. Triple-transfected cells demonstrated cyan and yellow fluorescence, as well as vacuolation. Donor filter (436-nm/20-nm band-pass excitation, 455-nm dichroic long-pass, and 480-nm/40-nm band-pass emission), acceptor filter (500-nm/20-nm band-pass excitation, 515-nm dichroic long-pass, and 535-nm/30-nm band-pass emission), and FRET filter (436-nm/20-nm band-pass excitation, 455-nm dichroic long-pass, and 535-nm/30-nm band-pass emission) cubes were used. An acceptor filter image was captured first and was then immediately switched to the donor and FRET filters without changing the field, using an exposure time of 1.6 s. Images were converted to grayscale, and the image was inverted (to obtain positive values from pixel analysis) using Adobe Photoshop. Single HeLa cells for the acceptor filter image were selected using Image Gauge 3.0 software. The same frame was selected by coordinate in the acceptor, donor, and FRET images, and pixel counts were determined. The FRET signal was calculated using $FRET_N$ (24). $FRET_N = Ff - Df(Fd/Dd) - Af(Fa/Aa)$ where F = both fluors present in the same cell, D = only the donor fluor present, A = only the acceptor fluor present, f = fluor(s) viewed under the FRET filter, d = fluor(s) viewed under the donor filter, and a = fluor(s) viewed under the acceptor filter. Because no cross talk exists between the fluors used (CFP is not visible in the YFP filter and YFP is not visible in the CFP filter), the $FRET_N$ denominator does not apply. For a full treatment, see Gordon et al. (24). This equation corrects for the background signal observed in the absence of FRET.

Confocal microscopy. HeLa cells were seeded on eight-well Lab-Tek chamber slides at 5×10^4 cells/ml and 400 μl/well and were grown overnight at 37°C under 5% CO_2. VacA-GFP and a VacA fusion protein containing the Ha (VacA-HA) affinity recognition sequence were coexpressed within cotransfected HeLa cells at 37°C, as described above in "Mammalian cell transfection." After 18 h, cells were fixed in 4% paraformaldehyde in PBS for 20 min, rinsed with PBS, and permeabilized with 0.2% Triton X-100 for 10 min. At room temperature, the monolayers were washed three times with PBS and incubated with blocking buffer (1% bovine serum albumin in PBS) for 1 h, followed by 60 min of incubation with 5 μg of monoclonal anti-HA (Sigma, St. Louis, Mo.)/ml, also at room temperature. The monolayers were then washed three times with PBS and incubated with 1:100 anti-mouse–horseradish peroxidase conjugate in blocking buffer for 30 min at room temperature. For detection of VacA-HA, we used the triamide signal amplification kit with Alexa Fluor 568 according to the manufacturer's specifications. Images were collected on a Zeiss (Thornwood, N.Y.) LSM 310 confocal microscope with an Omnichrome (Melles Griot, Irvine, Calif.) external Ar/Kr ion laser. GFP and Alexa Fluor 568 were captured using excitation lasers at 488 or 568 nm and were detected using 515- to 565-nm band-pass and 590-nm long-pass filters, respectively, with ×400 magnification at 4× zoom.

Statistical analysis. Data analyses were conducted using Student's paired *t* test. A *P* value of less than 0.05 is considered statistically significant.

RESULTS

We initially used FRET microscopy to investigate potential interactions between the two fragments of VacA, p37 and p58. As discrete fragments, p37 and p58 are inactive (14, 15, 65). However, these two fragments complement the vacuolating activity of full-length VacA when coexpressed within mammalian cells (65). While we hypothesize that p37 and p58 function in *trans* by directly associating, it is also possible that these two fragments act at two independent sites within the cell to carry out discrete biochemical activities, both of which are essential to induce vacuolation of intoxicated cells. We earlier established that carboxyl-terminal GFP fusions to either p37 (p37-GFP) or p58 (p58-GFP) did not block the ability of these two fragments to function in *trans* (65), suggesting that fusion proteins would be powerful probes for studying whether these domains interact within living cells, where VacA exerts its cytotoxic effects.

In preliminary experiments, we investigated the possibility that GFP could mediate interactions between p37 and p58. Immunoprecipitation experiments were performed using ^{35}S-radiolabeled forms of p37, p58, and GFP produced by in vitro transcription and translation. p58-GFP was incubated with an equimolar amount of p37 tagged at the amino terminus with the HA affinity peptide (HA-p37), revealing that the carboxyl-terminal GFP fusion did not prevent p58-GFP from interacting with HA-p37 (Fig. 1A). In addition, neither p37 (Fig. 1A) nor p58 (data not shown) directly interacted with GFP alone, indicating that the carboxyl-terminal GFP did not mediate associations between p37 and p58. Collectively, these preliminary experiments indicated that, at least in vitro, GFP fusions neither interfere with nor mediate interactions between p37 and p58.

To investigate whether p37 and p58 directly associate within vacuolated cells, we performed FRET microscopy analysis of transiently transfected HeLa cells, as previously described (14, 65). HeLa cells were first infected with vaccinia virus expressing recombinant T7 RNA polymerase and were subsequently transfected with pET20b and pET26b plasmids bearing VacA fusion genes under control of the T7 promoter. After 18 to 24 h, digital images of single cells were captured under YFP (excitation at 500 nm and emission at 535 nm), CFP (excitation at 436 nm and fluorescence emission at 480 nm), and FRET (excitation at 436 nm and emission at 535 nm) filter sets. The images were quantified by pixel analysis, and the FRET signal was obtained using the $FRET_N$ equation (24). In control experiments, cells expressing YFP-CFP fusion proteins demonstrated a significantly enhanced FRET signal relative to cells expressing YFP and CFP as discrete proteins (Fig. 1B), which have been shown not to interact (39).

Monolayers of HeLa cells were cotransfected with plasmids encoding p37-CFP and p58-YFP (14, 65). After 24 h, the monolayers were analyzed both for vacuolation and for interactions between p37-CFP and p58-YFP. Vacuolation was quantified by measuring the ability of vacuolated cells to take up the acidotrophic dye neutral red to a greater extent than nonvacuolated cells could, as previously described (8). Coexpression of p37-CFP and p58-YFP resulted in greatly enhanced uptake of neutral red relative to monolayers expressing either of the two fusion proteins alone (data not shown), confirming that these two fusion proteins were able to function in *trans* to induce vacuolation, as previously described (65). When the HeLa cell monolayers were analyzed by fluorescence microscopy, we found that cells coexpressing both p37-CFP and p58-YFP yielded a significantly enhanced FRET signal relative to cells expressing p37-CFP and YFP, or alternatively, p58-YFP and CFP (Fig. 1C). Notably, only those cells that were vacuolated yielded FRET. Collectively, these data demonstrate, for the first time, direct association between p37 and p58 within vacuolated cells.

VacA monomers associate within vacuolated cells. To investigate the structure of VacA within vacuolated cells, carboxyl-terminal fusions of VacA to either CFP or YFP (VacA-CFP or VacA-YFP, respectively) were expressed within HeLa cells. After 24 h, the cells were analyzed by FRET microscopy. These data revealed that cells coexpressing VacA-YFP and VacA-CFP yielded a much greater FRET signal than did cells expressing VacA-YFP and CFP or VacA-CFP and YFP (Fig. 2A), indicating that VacA monomers associate within the cytosol of transfected cells. Notably, monolayers coexpressing VacA-CFP and VacA-YFP were vacuolated to the same extent as cells expressing VacA alone, as revealed by the uptake of neutral red (data not shown), which correlates the presence of monomer interactions to the vacuolation of cells. The results from the FRET microscopy experiments were consistent with in vitro immunoprecipitation experiments using ^{35}S-radiolabeled VacA fusion proteins (Fig. 2B). VacA-GFP immunoprecipitated with HA-VacA (Fig. 2B), further confirming that a carboxyl-terminal GFP fusion does not interfere with the ability of a VacA monomer to associate with another monomer. Moreover, GFP did not coimmunoprecipitate with HA-VacA, indicating that GFP does not interact with VacA, and is therefore not responsible for mediating interactions between VacA monomers. To rule out the possibility that GFP-based fusions alter VacA cellular targeting, we used confocal microscopy to investigate the localization of VacA-GFP within cells coexpressing HA-VacA. These experiments clearly indicated that VacA-GFP and HA-VacA colocalize within mammalian cells (Fig. 2C).

Inactive VacA point mutants interact with but do not neutralize wild-type VacA. The demonstration that VacA monomers associate within vacuolated cells suggested that FRET microscopy would be a powerful approach for investigating the

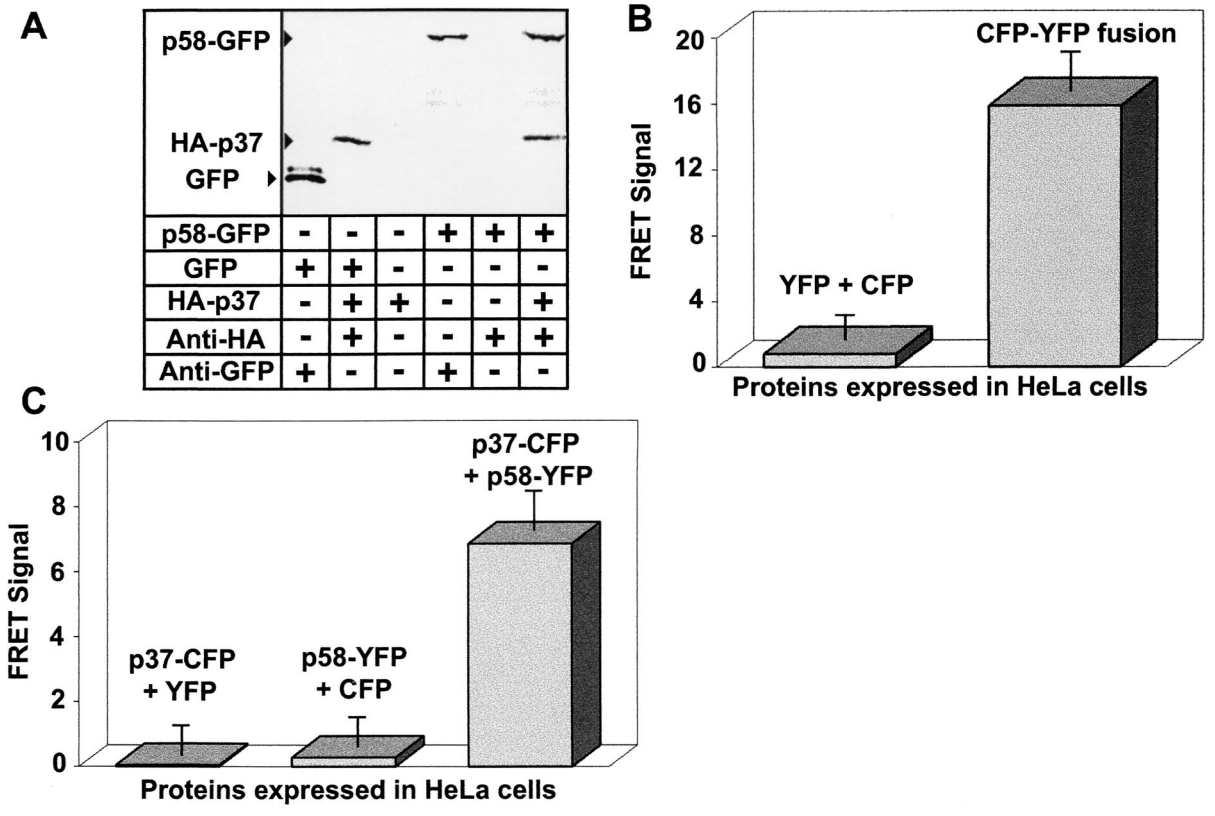

FIG. 1. VacA domain interactions. (A) In vitro interactions. ^{35}S-radiolabeled HA-p37, HA-p58, p37-GFP, p58-GFP, and GFP were synthesized by in vitro transcription and translation as described in Materials and Methods. Equimolar concentrations (0.5 nM) of the indicated recombinant proteins were added to Eppendorf tubes and were incubated for 1 h at 37°C in PBS, pH 7.2 (final volume, 500 μl). The protein mixtures were then incubated with 10 μl of protein G agarose beads in the presence (+) or absence (−) of 5 μl of the indicated antibodies for 30 min. After incubation, the beads were washed five times with 500 μl of 20 mM Tris, pH 8.0, 25 mM NaCl, and 0.2% Tween 20. The bound proteins were dissociated from the beads by denaturation in sample buffer and resolved on SDS–12% PAGE. The gel was dried and exposed to a phosphorimaging plate overnight. (B) FRET positive and negative controls. HeLa cells were infected with vT7 and were then transfected with plasmids expressing the indicated fluorescent proteins as described in Materials and Methods. After 18 to 24 h, the fluorescence emission of the transfected cells was analyzed by fluorescence microscopy. Images were collected for each slide using a CFP filter set (excitation at 436 nm and fluorescence emission at 480 nm), a YFP filter set (excitation at 500 nm and emission at 535 nm), and a FRET filter set (excitation at 436 nm and emission at 535 nm). Fluorescence images were collected for cells cotransfected with plasmids encoding CFP and YFP separately (left) or the CFP-YFP fusion positive control (right). The data were manipulated as described in the text. Values represent the average of at least 12 independent cells and 3 independent experiments. (C) p37 and p58 interact in *trans*. HeLa cells were infected with vT7 and were then cotransfected with plasmids expressing the indicated fluorescent protein fusions as described in Materials and Methods. After 18 to 24 h, images were collected and processed as described in Materials and Methods and for panel B above. Values represent the average of at least 12 independent cells and 3 independent experiments.

effects of inactivating mutations on toxin interactions. Previous efforts to map VacA determinants important for toxin activity have revealed that the VacA amino terminus is especially susceptible to inactivating mutations (59, 64). In particular, scientists have identified the first two single-amino-acid substitutions that inactivate the toxin activity, which are alanine substitutions for proline-9 (VacA [P9A]) and glycine-14 (VacA [G14A]) (64). McClain and coworkers (35) further showed that the amino terminus of VacA (G14A) was defective in a protein fusion reporter assay, based on the ability of discrete monomers to interact within a lipid bilayer, which led to the proposal that the VacA amino terminus may mediate interactions between discrete monomers. To test this hypothesis, we coexpressed VacA (G14A)-CFP and VacA (P9A)-YFP within HeLa cells. VacA (G14A)-CFP and VacA (G14A)-YFP were clearly devoid of cellular vacuolating activity (data not shown), in agreement with previous results (64). However, FRET microscopy analysis revealed that cells coexpressing VacA (G14A)-CFP and VacA (G14A)-YFP demonstrated a FRET signal similar to that of cells coexpressing VacA-CFP and VacA-YFP (Fig. 3). Essentially identical results were also found in experiments in which VacA (P9A)-CFP and VacA (P9A)-YFP were coexpressed within HeLa cells (Fig. 3). Collectively, these data indicate that, although mutations in the amino terminus are sufficient to eliminate toxin vacuolating activity, they do not eliminate the ability of monomers to associate. These results provided the opportunity to investigate whether the elevated FRET signal detected in cells expressing CFP and YFP fusions of VacA are derived from specific or nonspecific interactions between VacA monomers. In triple-transfection experiments, we expressed unlabeled p37 along with VacA (P9A)-CFP and VacA (P9A)-YFP. In these experiments, CFP and YFP fluorescence indicated the expression of VacA (P9A)-CFP and VacA (P9A)-YFP, while cellular vacu-

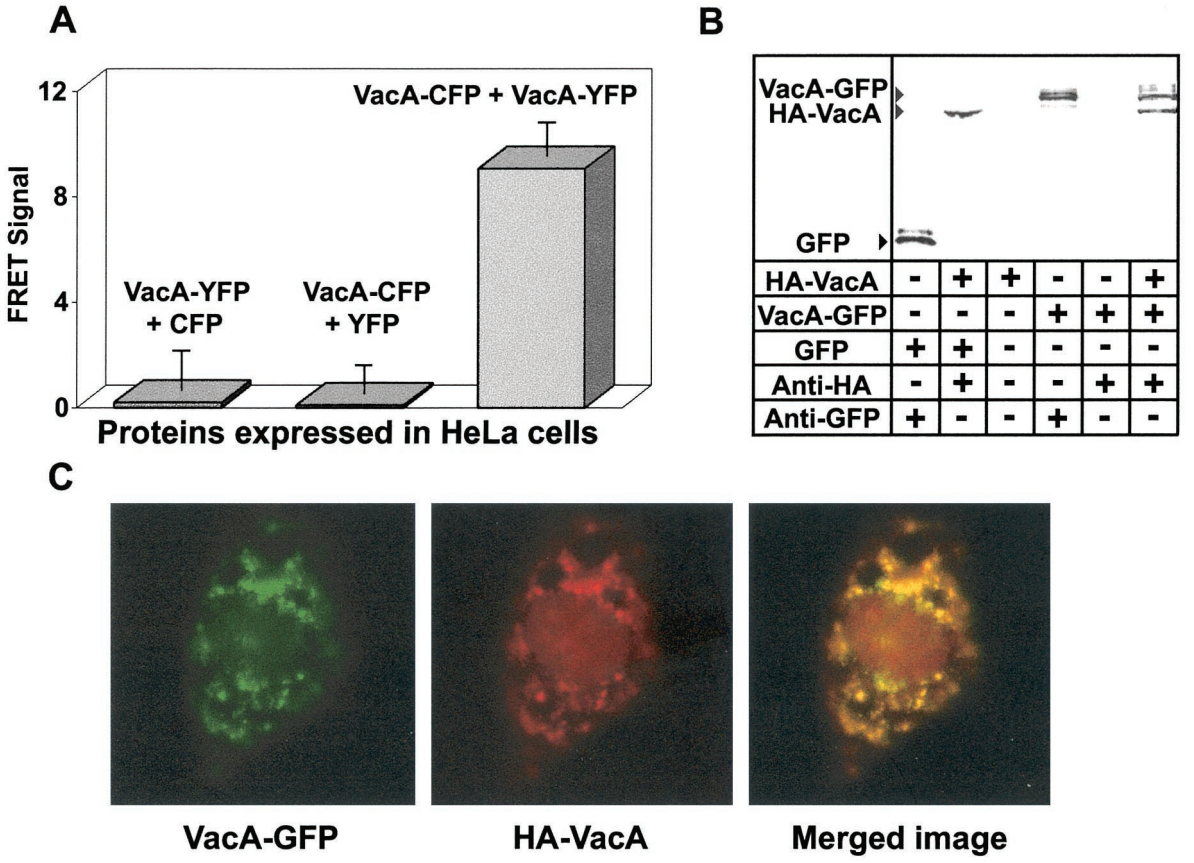

FIG. 2. VacA monomer interactions. (A) VacA monomers interact within the cytosol of HeLa cells. HeLa cells were cotransfected with plasmids expressing VacA genetically fused to either CFP or YFP, and FRET images were collected and analyzed as described for Fig. 1. Values represent the average of at least 12 independent cells and 3 independent experiments. (B) In vitro interactions. HA-VacA and VacA-GFP monomers or GFP control were synthesized, and immunoprecipitation experiments were conducted as described for Fig. 1. (C) HA-VacA and VacA-GFP colocalization. Confocal microscopy images were collected as described under Materials and Methods: VacA-GFP, HA-VacA, and overlay of images in panels 1 and 2 (Merged image).

olation indicated the expression of p37, which functionally complements VacA (P9A), as previously reported (66). Analysis of vacuolated cells demonstrated that unlabeled p37 decreased the detectable FRET signal relative to that from cells expressing VacA (P9A)-CFP and VacA (P9A)-YFP alone (Fig. 3), suggesting that p37 competitively inhibits the interaction between these two species. These data support the view that the elevated FRET signal obtained in cells expressing VacA fused to CFP and YFP is due to specific interactions between toxin monomers.

Because FRET microscopy revealed that monomers of VacA (P9A)-CFP and VacA (G14A)-YFP interact within cells, we next tested whether inactive monomers might interact with wild-type VacA and potentially block the vacuolation activity of the toxin. We coexpressed VacA-CFP and either VacA (G14A)-YFP or VacA (P9A)-YFP within HeLa. After 24 h, analysis of monolayer vacuolation revealed that cells coexpressing VacA-CFP and VacA (G14A)-YFP or VacA-CFP and VacA (P9A)-YFP took up the dye neutral red to the same extent that cells expressing VacA alone did (Fig. 4A). FRET microscopy analysis of the monolayers indicated that VacA-CFP readily interacted with either VacA (G14A)-YFP or VacA (P9A)-YFP (Fig. 4B). Collectively, these data indicate that, although wild-type VacA readily interacts with some mutant forms of the toxin with inactivating mutations, the formation of these complexes does not block the vacuolation of the HeLa cell monolayers.

Finally, we investigated a mutant form of the toxin, VacA Δ(6-26), which demonstrates a dominant-negative activity by blocking the ability of wild-type VacA to induce vacuolation of target cells (37, 59). We coexpressed VacA Δ(6-26)-YFP and either VacA-CFP or VacA Δ(6-26)-CFP. As previously reported, VacA Δ(6-26) was unable to induce vacuolation and readily blocked vacuolating activity when coexpressed with wild-type VacA (data not shown) (40). FRET microscopy analysis of the monolayers revealed that monomers of VacA Δ(6-26) interact (Fig. 5). Moreover, cells expressing both VacA Δ(6-26)-YFP and VacA-CFP demonstrated an enhanced FRET signal, supporting a model in which the dominant-negative activity of this mutant form of VacA originates from its ability to form mixed complexes with wild-type VacA that blocks the toxin's cellular vacuolating activity.

DISCUSSION

FRET microscopy was employed to probe the overall quaternary structure of both wild-type and mutant forms of VacA

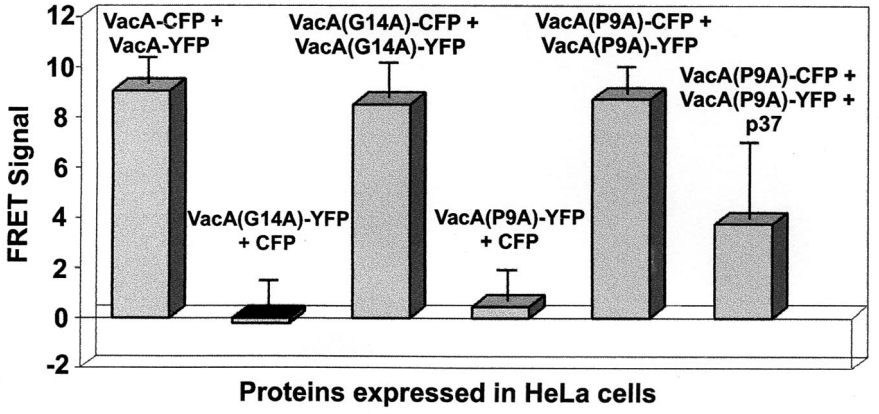

FIG. 3. Inactivating point mutations do not disrupt multimer formation. HeLa cells were infected with vT7 and were then cotransfected with plasmids expressing the indicated proteins as described in Materials and Methods. After 18 to 24 h, the fluorescence emission of the transfected cells was analyzed by fluorescence microscopy, and FRET images were collected and analyzed as described for Fig. 1. The data were manipulated as described in the text. Values represent the average of at least 12 independent cells and 3 independent experiments. For triple-transfected cells expressing VacA (P9A)-CFP, VacA (P9A)-YFP, and p37, $P < 0.001$ compared to that for cotransfected cells expressing VacA (P9A)-CFP and VacA (P9A)-YFP.

within mammalian cells. The power of FRET microscopy originates from the ability to analyze protein associations within the intracellular environment in which they function (47). Moreover, unlike two-hybrid systems, FRET microscopy does not require localization of the two protein partners to the nucleus, resulting in a nonphysiological environment to investigate protein interactions. FRET microscopy has been used to demonstrate association of calcium channels with calmodulin (18), show Bcl-2 interactions with Bax in the mitochondria (31), and examine SNARE complex interactions (62). This approach has been used to demonstrate that monomers of human TSH receptors associate within living cells (28), thus providing valuable information as to the quaternary structure of this protein. Collectively, these studies and others have indicated the power of FRET microscopy for intracellular studies of protein-protein interactions.

Our data indicate that VacA monomers associate within intact, vacuolated cells. To observe intracellular toxin associations, we expressed VacA directly within mammalian cells in order to bypass the binding and internalization steps of intoxication. In these studies, FRET microscopy demonstrated a clearly elevated FRET signal in cells expressing both VacA-CFP and VacA-YFP. In control experiments, these fluorescent protein fusions were not found to (i) facilitate the observed interactions between discrete VacA monomers, (ii) cause VacA to improperly localize within mammalian cells, or (iii) alter the specific nature of VacA monomer interactions. Collectively, these results support a model that VacA intracellular

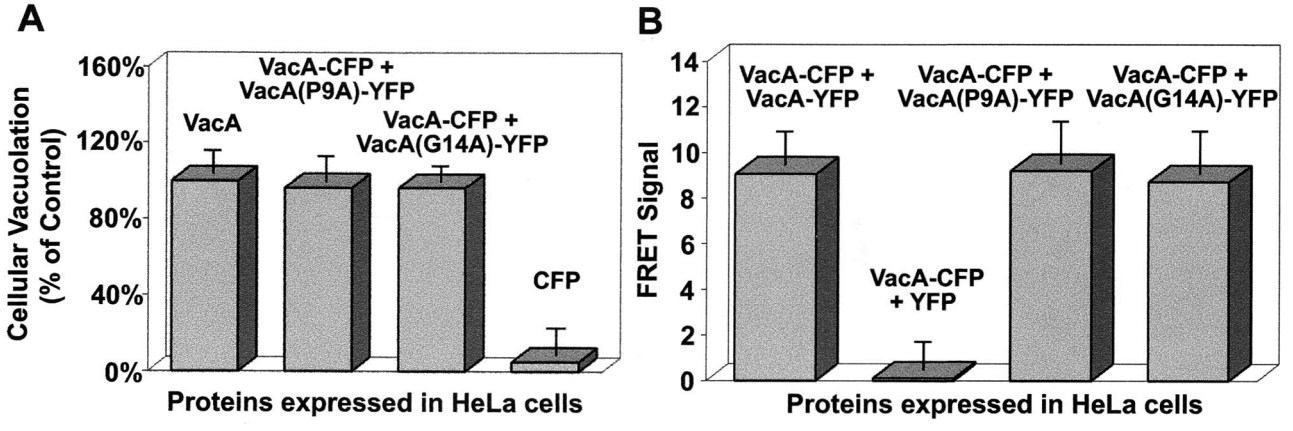

FIG. 4. Inactivating point mutations do not disrupt heteromultimer formation. (A) Cells expressing wild-type and mutant forms of VacA are vacuolated. HeLa cells were infected with vT7 and were then transfected with plasmids encoding the indicated protein or protein fusions as described in Materials and Methods. After 24 h, cells were analyzed for neutral red uptake and total protein, as described in Materials and Methods. Data were collected in triplicate for three independent experiments and are expressed relative to cells expressing VacA alone. (B) Wild-type and mutant forms of VacA associate within cells. HeLa cells were infected with vT7 and were then cotransfected with plasmids expressing the indicated fluorescent protein fusions as described in Materials and Methods. After 18 to 24 h, the fluorescence emission of the transfected cells was analyzed by fluorescence microscopy, and FRET images were collected and analyzed as described for Fig. 1. The data were manipulated as described in the text. Values represent the average of at least 12 independent cells and 3 independent experiments.

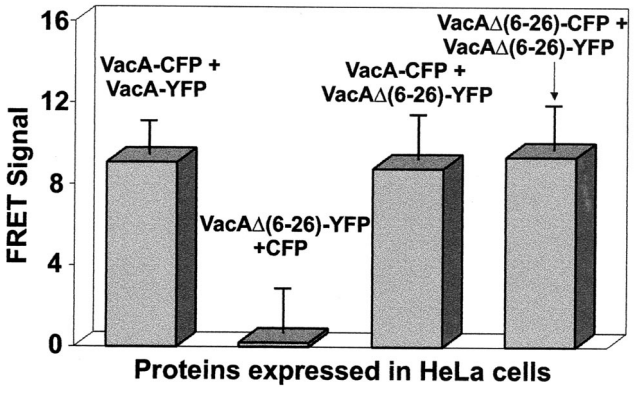

FIG. 5. VacA dominant-negative interactions. HeLa cells were infected with vT7 and were then cotransfected with plasmids expressing the indicated fluorescent protein fusions as described in Materials and Methods. After 18 to 24 h, the fluorescence emission of the transfected cells was analyzed by fluorescence microscopy, and FRET images were collected and analyzed as described for Fig. 1. The data were manipulated as described in the text. Values represent the average of at least 12 independent cells and 3 independent experiments.

vacuolating activity is mediated by toxin monomers associating at an intracellular location to form a higher-order complex.

Debate and alternative hypotheses have persisted as to the mechanism by which VacA induces cellular vacuolation. The similarity of VacA to members of the family of intracellularly acting toxins suggests that VacA, or a fragment of VacA, might catalytically modify an intracellular target regulating membrane trafficking (5, 57, 61). These active, intracellular forms of most of these toxins are believed to be monomers (19, 38, 41). On the other hand, it has been proposed that VacA induces vacuole formation directly through its ability to assemble into oligomers and form ion-conducting channels (42, 45, 58). VacA clearly forms higher-order structures in solution, as demonstrated by quantitative size exclusion chromatography, electron microscopy, and metal replicas (7, 27, 30, 50). While we could not determine whether VacA assembles into a structure resembling the hexameric and heptameric rings observed in vitro, results from our FRET microscopy experiments indicate that VacA monomers associate within vacuolated cells, consistent with the model holding that VacA functions as a higher-order complex. Moreover, while FRET microscopy cannot reveal the intracellular biochemical activity of VacA, these data provide a structural basis to support the model that VacA may form channels from within cells. We cannot rule out the possibility, however, that association of VacA monomers confers an alternative biochemical activity on the toxin.

The demonstration that VacA monomers directly associate within vacuolated cells provides an important assay to investigate the effects of mutations on toxin interactions. We investigated two known point mutations located within the VacA amino terminus that are known to inactivate toxin vacuolating activity (64). The VacA amino terminus is hydrophobic, and three tandem repeats of a GxxxG motif characteristic of transmembrane dimerization sequences were recently identified (35). The importance of this transmembrane region was analyzed using ToxR-VacA-maltose binding protein fusions to study transmembrane helix-helix associations in an *Escherichia coli* membrane environment. A wild-type VacA hydrophobic region (residues 1 to 32) mediated insertion of the fusion protein into the inner membrane of *E. coli* and mediated protein dimerization (35). Fusions of the mutant forms of the amino terminus also inserted into the inner membrane but were defective in dimerization. Based on these results, it was proposed that the wild-type VacA amino-terminal hydrophobic region contributes to oligomerization of the toxin within membranes of eukaryotic cells. To further test this hypothesis, we analyzed whether VacA (G14A) can associate within mammalian cells. FRET microscopy revealed that VacA (G14A), as well as VacA (P9A), was able to associate into higher-order forms, indicating that these inactivating point mutations within the amino terminus were not sufficient to block the associations between toxin monomers in mammalian cells. Because the experiments reported earlier with the ToxR-VacA-maltose binding protein fusions demonstrated that the alanine substitution at residue 14 attenuated interactions between these putative transmembrane segments (35), our data suggest that interactions between VacA monomers require determinants located outside the VacA amino terminus. Such a model predicts that monomers of VacA (G14A) retain the ability to associate but are inactivated by a defect in the putative transmembrane region located at the amino terminus. Our data also indicate that VacA (G14A) (as well as VacA [P9A]) interacts with wild-type toxin in a manner that did not result in a detectable decrease in cellular vacuolation. These results suggest that heterocomplexes comprising wild-type and mutant forms of VacA retain vacuolating activity. However, we cannot presently rule out a scenario in which VacA heterocomplexes are unable to induce vacuolation but in which the presence within the cell of a very small population of VacA homocomplexes comprising all wild-type monomers is sufficient to induce vacuolation of the entire cell.

A mutant form of VacA with a deletion of residues 6 to 26 (VacA Δ[6-26]) was earlier demonstrated to lack vacuolating activity, both when expressed intracellularly and when added exogenously to mammalian cells (59). In addition, coexpression of VacA Δ(6-26) with wild-type VacA within HeLa cell monolayers was found to block vacuolation of these cells, leading to the proposal that VacA Δ(6-26) demonstrated dominant-negative activity resulting from the formation of mixed oligomers between the mutant and wild-type VacA proteins with defective functional activity. However, it was not demonstrated that VacA Δ(6-26) associated with wild-type VacA intracellularly. FRET microscopy revealed that monomers of VacA Δ(6-26) associated with one another. Significantly, within cotransfected cells, we also demonstrated that VacA Δ(6-26) directly associated with wild-type VacA. These results strongly support the model that the intracellular dominant-negative activity of VacA Δ(6-26) may originate from its ability to associate with wild-type toxin in a manner that blocks intracellular activity. It will be of interest in the future to more precisely define the differences between the associations of VacA with VacA Δ(6-26), which blocks cellular vacuolation, and with VacA (G14A), which does not block toxin function as a heterocomplex.

Finally, we have demonstrated the usefulness of FRET microscopy for probing possible interactions between smaller fragments of the toxin. Our results clearly indicate that p37 and

p58, the two fragments of VacA, directly associate within mammalian cells. Because these two inactive fragments are able to complement the toxin's vacuolating activity (65), these data strongly suggest that p37 and p58 must associate to function in *trans*. This is the first demonstration that p37 and p58 directly associate within cells and would seem not to support the alternative possibility that these two fragments induce vacuolation by functioning independently within cells.

In summary, FRET microscopy has been used to investigate properties of VacA within the intracellular environment where the toxin elaborates its cytotoxicity. Because VacA monomers associate under conditions that result in cellular vacuolation, our data support a model holding that VacA functions as a protein complex comprising two or more toxin monomers. While many pore-forming toxins exert their effects as oligomeric structures at the plasma membrane, VacA may represent the first example of a toxin that exerts its effects intracellularly as a higher-order complex. In the future, as additional functional domains and subdomains of VacA are identified, FRET microscopy will provide a powerful approach for mapping determinants that are important for both inter- and intramolecular interactions from within the intracellular environment.

ACKNOWLEDGMENTS

We thank P. Hardin for the use of a fluorescence microscope and also thank A. Vailas and D. Martinez, who provided access to their laboratory's microtiter plate reader.

This work was supported by the National Institutes of Health (RO1 AI45928), the Robert A. Welch Foundation (E-1311), and the American Heart Association (98BG472).

REFERENCES

1. **Atherton, J. C., P. Cao, R. M. Peek, Jr., M. K. Tummuru, M. J. Blaser, and T. L. Cover.** 1995. Mosaicism in vacuolating cytotoxin alleles of Helicobacter pylori. Association of specific vacA types with cytotoxin production and peptic ulceration. J. Biol. Chem. **270:**17771–17777.
2. **Blaser, M. J.** 1993. Helicobacter pylori: microbiology of a 'slow' bacterial infection. Trends Microbiol. **1:**255–260.
3. **Catrenich, C. E., and M. H. Chestnut.** 1992. Character and origin of vacuoles induced in mammalian cells by the cytotoxin of Helicobacter pylori. J. Med. Microbiol. **37:**389–395.
4. **Censini, S., C. Lange, Z. Xiang, J. E. Crabtree, P. Ghiara, M. Borodovsky, R. Rappuoli, and A. Covacci.** 1996. cag, a pathogenicity island of Helicobacter pylori, encodes type I-specific and disease-associated virulence factors. Proc. Natl. Acad. Sci. USA **93:**14648–14653.
5. **Cover, T. L.** 1996. The vacuolating cytotoxin of Helicobacter pylori. Mol. Microbiol. **20:**241–246.
6. **Cover, T. L., and M. J. Blaser.** 1996. Helicobacter pylori infection, a paradigm for chronic mucosal inflammation: pathogenesis and implications for eradication and prevention. Adv. Intern. Med. **41:**85–117.
7. **Cover, T. L., and M. J. Blaser.** 1992. Purification and characterization of the vacuolating toxin from Helicobacter pylori. J. Biol. Chem. **267:**10570–10575.
8. **Cover, T. L., S. A. Halter, and M. J. Blaser.** 1992. Characterization of HeLa cell vacuoles induced by Helicobacter pylori broth culture supernatant. Hum. Pathol. **23:**1004–1010.
9. **Cover, T. L., P. I. Hanson, and J. E. Heuser.** 1997. Acid-induced dissociation of VacA, the Helicobacter pylori vacuolating cytotoxin, reveals its pattern of assembly. J. Cell Biol. **138:**759–769.
10. **Cover, T. L., W. Puryear, G. I. Perez-Perez, and M. J. Blaser.** 1991. Effect of urease on HeLa cell vacuolation induced by *Helicobacter pylori* cytotoxin. Infect. Immun. **59:**1264–1270.
11. **Cover, T. L., M. K. Tummuru, P. Cao, S. A. Thompson, and M. J. Blaser.** 1994. Divergence of genetic sequences for the vacuolating cytotoxin among Helicobacter pylori strains. J. Biol. Chem. **269:**10566–10573.
12. **Cover, T. L., S. G. Vaughn, P. Cao, and M. J. Blaser.** 1992. Potentiation of Helicobacter pylori vacuolating toxin activity by nicotine and other weak bases. J. Infect. Dis. **166:**1073–1078.
13. **Day, R. N., A. Periasamy, and F. Schaufele.** 2001. Fluorescence resonance energy transfer microscopy of localized protein interactions in the living cell nucleus. Methods **25:**4–18.
14. **de Bernard, M., B. Arico, E. Papini, R. Rizzuto, G. Grandi, R. Rappuoli, and C. Montecucco.** 1997. Helicobacter pylori toxin VacA induces vacuole formation by acting in the cell cytosol. Mol. Microbiol. **26:**665–674.
15. **de Bernard, M., D. Burroni, E. Papini, R. Rappuoli, J. Telford, and C. Montecucco.** 1998. Identification of the *Helicobacter pylori* VacA toxin domain active in the cell cytosol. Infect. Immun. **66:**6014–6016.
16. **de Bernard, M., M. Moschioni, G. Napolitani, R. Rappuoli, and C. Montecucco.** 2000. The VacA toxin of Helicobacter pylori identifies a new intermediate filament-interacting protein. EMBO J. **19:**48–56.
17. **de Bernard, M., E. Papini, V. de Filippis, E. Gottardi, J. Telford, R. Manetti, A. Fontana, R. Rappuoli, and C. Montecucco.** 1995. Low pH activates the vacuolating toxin of Helicobacter pylori, which becomes acid and pepsin resistant. J. Biol. Chem. **270:**23937–23940.
18. **Erickson, M. G., B. A. Alseikhan, B. Z. Peterson, and D. T. Yue.** 2001. Preassociation of calmodulin with voltage-gated Ca(2+) channels revealed by FRET in single living cells. Neuron **31:**973–985.
19. **Falnes, P. O., and K. Sandvig.** 2000. Penetration of protein toxins into cells. Curr. Opin. Cell Biol. **12:**407–413.
20. **Fuerst, T. R., E. G. Niles, F. W. Studier, and B. Moss.** 1986. Eukaryotic transient-expression system based on recombinant vaccinia virus that synthesizes bacteriophage T7 RNA polymerase. Proc. Natl. Acad. Sci. USA **83:**8122–8126.
21. **Galmiche, A., J. Rassow, A. Doye, S. Cagnol, J. C. Chambard, S. Contamin, V. de Thillot, I. Just, V. Ricci, E. Solcia, E. Van Obberghen, and P. Boquet.** 2000. The N-terminal 34 kDa fragment of Helicobacter pylori vacuolating cytotoxin targets mitochondria and induces cytochrome c release. EMBO J. **19:**6361–6370.
22. **Garner, J. A., and T. L. Cover.** 1996. Binding and internalization of the *Helicobacter pylori* vacuolating cytotoxin by epithelial cells. Infect. Immun. **64:**4197–4203.
23. **Ghiara, P., M. Marchetti, M. J. Blaser, M. K. Tummuru, T. L. Cover, E. D. Segal, L. S. Tompkins, and R. Rappuoli.** 1995. Role of the *Helicobacter pylori* virulence factors vacuolating cytotoxin, CagA, and urease in a mouse model of disease. Infect. Immun. **63:**4154–4160.
24. **Gordon, G. W., G. Berry, X. H. Liang, B. Levine, and B. Herman.** 1998. Quantitative fluorescence resonance energy transfer measurements using fluorescence microscopy. Biophys. J. **74:**2702–2713.
25. **Hennig, E. E., E. Butruk, and J. Ostrowski.** 2001. RACK1 protein interacts with Helicobacter pylori VacA cytotoxin: the yeast two-hybrid approach. Biochem. Biophys. Res. Commun. **289:**103–110.
26. **Kuck, D., B. Kolmerer, C. Iking-Konert, P. H. Krammer, W. Stremmel, and J. Rudi.** 2001. Vacuolating cytotoxin of *Helicobacter pylori* induces apoptosis in the human gastric epithelial cell line AGS. Infect. Immun. **69:**5080–5087.
27. **Lanzavecchia, S., P. L. Bellon, P. Lupetti, R. Dallai, R. Rappuoli, and J. L. Telford.** 1998. Three-dimensional reconstruction of metal replicas of the Helicobacter pylori vacuolating cytotoxin. J. Struct. Biol. **121:**9–18.
28. **Latif, R., P. Graves, and T. F. Davies.** 2001. Oligomerization of the human TSH receptor: fluorescent protein-tagged hTSHR reveals post-translational complexes. J. Biol. Chem. **276:**45217–45224.
29. **Leunk, R., P. Johnson, B. David, W. Kraft, and D. Morgan.** 1988. Cytotoxin activity in broth culture filtrates of *Campylobacter pylori*. J. Med. Microbiol. **26:**93–99.
30. **Lupetti, P., J. E. Heuser, R. Manetti, P. Massari, S. Lanzavecchia, P. L. Bellon, R. Dallai, R. Rappuoli, and J. L. Telford.** 1996. Oligomeric and subunit structure of the Helicobacter pylori vacuolating cytotoxin. J. Cell Biol. **133:**801–807.
31. **Mahajan, N. P., K. Linder, G. Berry, G. W. Gordon, R. Heim, and B. Herman.** 1998. Bcl-2 and Bax interactions in mitochondria probed with green fluorescent protein and fluorescence resonance energy transfer. Nat. Biotechnol. **16:**547–552.
32. **Marchetti, M., B. Arico, D. Burroni, N. Figura, R. Rappuoli, and P. Ghiara.** 1995. Development of a mouse model of Helicobacter pylori infection that mimics human disease. Science **267:**1655–1658.
33. **Marshall, B. J., J. A. Armstrong, D. B. McGechie, and R. J. Glancy.** 1985. Attempt to fulfil Koch's postulates for pyloric Campylobacter. Med. J. Aust. **142:**436–439.
34. **Marshall, B. J., and J. R. Warren.** 1984. Unidentified curved bacilli in the stomach of patients with gastritis and peptic ulceration. Lancet **i:**1311–1315.
35. **McClain, M., P. Cao, and T. Cover.** 2001. Amino-terminal hydrophobic region of *Helicobacter pylori* vacuolating cytotoxin (VacA) mediates transmembrane protein dimerization. Infect. Immun. **69:**1181–1184.
36. **McClain, M., W. Schraw, V. Ricci, P. Boquet, and T. Cover.** 2000. Acid activation of Helicobacter pylori vacuolating cytotoxin (VacA) results in toxin internalization by eukaryotic cells. Mol. Microbiol. **37:**422–442.
37. **McClain, M. S., P. Cao, H. Iwamoto, A. D. Vinion-Dubiel, G. Szabo, Z. Shao, and T. L. Cover.** 2001. A 12-amino-acid segment, present in type s2 but not type s1 *Helicobacter pylori* VacA proteins, abolishes cytotoxin activity and alters membrane channel formation. J. Bacteriol. **183:**6499–6508.
38. **Menestrina, G., G. Schiavo, and C. Montecucco.** 1994. Molecular mechanisms of action of bacterial protein toxins. Mol. Aspects Med. **15:**79–193.
39. **Miyawaki, A., J. Llopis, R. Heim, J. M. McCaffery, J. A. Adams, M. Ikura,**

and R. Y. Tsien. 1997. Fluorescent indicators for Ca2+ based on green fluorescent proteins and calmodulin. Nature **388:**882–887.
40. **Montecucco, C., E. Papini, M. de Bernard, and M. Zoratti.** 1999. Molecular and cellular activities of Helicobacter pylori pathogenic factors. FEBS Lett. **452:**16–21.
41. **Montecucco, C., E. Papini, and G. Schiavo.** 1994. Bacterial protein toxins penetrate cells via a four-step mechanism. FEBS Lett. **346:**92–98.
42. **Morbiato, L., F. Tombola, S. Campello, G. Del Giudice, R. Rappuoli, M. Zoratti, and E. Papini.** 2001. Vacuolation induced by VacA toxin of Helicobacter pylori requires the intracellular accumulation of membrane permeant bases, Cl(-) and water. FEBS Lett. **508:**479–483.
43. **Nomura, A., G. N. Stemmermann, P. H. Chyou, I. Kato, G. I. Perez-Perez, and M. J. Blaser.** 1991. Helicobacter pylori infection and gastric carcinoma among Japanese Americans in Hawaii. N. Engl. J. Med. **325:**1132–1136.
44. **Pagliaccia, C., M. de Bernard, P. Lupetti, X. Ji, D. Burroni, T. L. Cover, E. Papini, R. Rappuoli, J. L. Telford, and J. M. Reyrat.** 1998. The m2 form of the Helicobacter pylori cytotoxin has cell type-specific vacuolating activity. Proc. Natl. Acad. Sci. USA **95:**10212–10217.
45. **Papini, E., M. Zoratti, and T. L. Cover.** 2001. In search of the Helicobacter pylori VacA mechanism of action. Toxicon **39:**1757–1767.
46. **Parsonnet, J., S. Hansen, L. Rodriguez, A. B. Gelb, R. A. Warnke, E. Jellum, N. Orentreich, J. H. Vogelman, and G. D. Friedman.** 1994. Helicobacter pylori infection and gastric lymphoma. N. Engl. J. Med. **330:**1267–1271.
47. **Pelicic, V., J. M. Reyrat, L. Sartori, C. Pagliaccia, R. Rappuoli, J. L. Telford, C. Montecucco, and E. Papini.** 1999. Helicobacter pylori VacA cytotoxin associated with the bacteria increases epithelial permeability independently of its vacuolating activity. Microbiology **145:**2043–2050.
48. **Periasamy, A.** 2001. Fluorescence resonance energy transfer microscopy: a mini review. J. Biomed. Opt. **6:**287–291.
49. **Phadnis, S., D. Ilver, L. Janson, S. Normark, and T. Westblom.** 1994. Essential role of urease in pathogenesis of gastritis induced by *Helicobacter pylori* in gnotobiotic piglets. Infect. Immun. **62:**1557–1565.
50. **Reyrat, J. M., R. Rappuoli, and J. L. Telford.** 2000. A structural overview of the Helicobacter cytotoxin. Int. J. Med. Microbiol. **290:**375–379.
51. **Ricci, V., A. Galmiche, A. Doye, V. Necchi, E. Solcia, and P. Boquet.** 2000. High cell sensitivity to Helicobacter pylori VacA toxin depends on a GPI-anchored protein and is not blocked by inhibition of the clathrin-mediated pathway of endocytosis. Mol. Biol. Cell **11:**3897–3909.
52. **Ricci, V., P. Sommi, R. Fiocca, N. Figura, M. Romano, K. Ivey, E. Solcia, and U. Ventura.** 1993. Cytotoxicity of *Helicobacter pylori* on human gastric epithelial cells *in vitro*: role of cytotoxin(s) and ammonia. Eur. J. Gastroenterol. Hepatol. **5:**687–694.
53. **Salama, N. R., G. Otto, L. Tompkins, and S. Falkow.** 2001. Vacuolating cytotoxin of *Helicobacter pylori* plays a role during colonization in a mouse model of infection. Infect. Immun. **69:**730–736.
54. **Sambrook, J., and D. Russell.** 2001. Molecular cloning: a laboratory manual, 3rd ed. Cold Spring Harbor Laboratory Press, Cold Spring Harbor, N.Y.
55. **Schmitt, W., and R. Haas.** 1994. Genetic analysis of the Helicobacter pylori vacuolating cytotoxin: structural similarities with the IgA protease type of exported protein. Mol. Microbiol. **12:**307–319.
56. **Sommi, P., V. Ricci, R. Fiocca, V. Necchi, M. Romano, J. L. Telford, E. Solcia, and U. Ventura.** 1998. Persistence of Helicobacter pylori VacA toxin and vacuolating potential in cultured gastric epithelial cells. Am. J. Physiol. **275:**G681–G688.
57. **Telford, J. L., P. Ghiara, M. Dell'Orco, M. Comanducci, D. Burroni, M. Bugnoli, M. F. Tecce, S. Censini, A. Covacci, Z. Xiang, et al.** 1994. Gene structure of the Helicobacter pylori cytotoxin and evidence of its key role in gastric disease. J. Exp. Med. **179:**1653–1658.
58. **Tombola, F., C. Pagliaccia, S. Campello, J. L. Telford, C. Montecucco, E. Papini, and M. Zoratti.** 2001. How the loop and middle regions influence the properties of Helicobacter pylori VacA channels. Biophys. J. **81:**3204–3215.
59. **Vinion-Dubiel, A. D., M. S. McClain, D. M. Czajkowsky, H. Iwamoto, D. Ye, P. Cao, W. Schraw, G. Szabo, S. R. Blanke, Z. Shao, and T. L. Cover.** 1999. A dominant negative mutant of Helicobacter pylori vacuolating toxin (VacA) inhibits VacA-induced cell vacuolation. J. Biol. Chem. **274:**37736–37742.
60. **Wang, H. J., and W. C. Wang.** 2000. Expression and binding analysis of GST-vacA fusions reveals that the C-terminal approximately 100-residue segment of exotoxin is crucial for binding in HeLa cells. Biochem. Biophys. Res. Commun. **278:**449–454.
61. **Willhite, D., A. Gutierrez, D. Ye, C. Williams, H. Patel, K. Marty, and S. Blanke.** 2000. Intracellular life and times of the *Helicobacter pylori* vacuolating toxin. SAAS Bull. Biochem. Biotechnol. **13:**35–53.
62. **Xia, Z., Q. Zhou, J. Lin, and Y. Liu.** 2001. Stable SNARE complex prior to evoked synaptic vesicle fusion revealed by fluorescence resonance energy transfer. J. Biol. Chem. **276:**1766–1771.
63. **Yahiro, K., T. Niidome, M. Kimura, T. Hatakeyama, H. Aoyagi, H. Kurazono, K. Imagawa, A. Wada, J. Moss, and T. Hirayama.** 1999. Activation of Helicobacter pylori VacA toxin by alkaline or acid conditions increases its binding to a 250-kDa receptor protein-tyrosine phosphatase beta. J. Biol. Chem. **274:**36693–36699.
64. **Ye, D., and S. R. Blanke.** 2000. Mutational analysis of the *Helicobacter pylori* vacuolating toxin amino terminus: identification of amino acids essential for cellular vacuolation. Infect. Immun. **68:**4354–4357.
65. **Ye, D., D. C. Willhite, and S. R. Blanke.** 1999. Identification of the minimal intracellular vacuolating domain of the Helicobacter pylori vacuolating toxin. J. Biol. Chem. **274:**9277–9282.
66. **Ye, D., and S. R. Blanke.** 2002. Functional complementation reveals the importance of intermolecular monomer interactions for Helicobacter pylori VacA vacuolating activity. Mol. Microbiol. **43:**1243–1253.

Editor: D. L. Burns